

Computational Investigation of Aerodynamic Characteristics for Elliptic UAV Wing

Amaal Attia¹, Ibrahim Elbadawy^{*1,2}, Osama E. Mahmoud¹

¹Mechanical Power Engineering Department, Faculty of Engineering - Mattaria, Helwan University, Cairo 11718, Egypt

²Department of Mechanical Engineering, College of Engineering and Technology, American University of the Middle East, Kuwait

Abstract

Unmanned Aerial Vehicles, UAVs, gained an important role in modern military and civilian applications. Developments in UAVs technology improve its performance and maneuverability with acceptable cost. Elliptic airfoil had been widely used in the development of Rotor/Wing subsonic aircraft. The present work aims to investigate the effect of various elliptic airfoil parameters, such as Reynolds number, angle of attack and airfoil thickness, on aerodynamic behavior using two-dimensional computational study. The computational results were validated by experimental results. Angles of attack was evaluated from 0° to 18° in order to analyze aerodynamic characteristics up to stall condition, while Reynolds number was evaluated at values of 1×10^5 , 3×10^5 , 2×10^6 , and 8×10^6 , to cover the range of rotary and fixed wing flight conditions. Thickness ratio was ranged from 5% to 25% to include the UAVs airfoil thicknesses so that choice best thickness gets maximum lift to drag ratio. In addition, the maximum thicknesses location was evaluated for a range of 30% to 70% to get suitable location gets maximum left to drag ratio. The ANSYS-Fluent software was used with Spalart-Allmaras turbulence model, and found that the maximum lift to drag ratio which improve the UAV capability in this study is at $Re=2 \times 10^6$, angle of attack at 8°, max thickness ratio of (0.1chord) located at (0.3chord).

Keywords: UAV; Elliptic airfoil; Aerodynamics.

1 Introduction

In recent times, UAVs have witnessed remarkable development as a result of increased confidence in the military and civilian applications. An unmanned vehicle with vertical take-off and landing (VTOL) ability represents one example of an interest area, which has possibility for important research innovation. A canard rotor/wing (CRW) is a UAV that falls under this category. CRWs can hover and fly at low speeds like a conventional helicopter and can also fly at high speeds like a fixed wing aircraft with the additional capability of VTOL. **Pandya and Aftosmis(2001)** This specific ability of CRWs to transform into various flight modes gives it importance for military and civilian applications and if it have an elliptical wing, it will do this property efficiently, and as a result of that importance of VTOL UAVs and elliptical wings, computational and experimental investigations have been carried out by many researchers.

The two pair of elliptical and circular shaped winglets with the wing of the aircraft model was described by **Hossain et al. (2007)** for the reduction of induced drag purpose without increasing the span of the aircraft. Aerodynamic characteristics for the aircraft model with and without winglet having wing with NACA section No. 65-3-218 has been studied using a subsonic wind tunnel of $1\text{m} \times 1\text{m}$ rectangular test section at the Reynolds numbers of 0.17×10^6 , 0.21×10^6 and 0.25×10^6 . Elliptical winglet at 60° incidence angle has the better performance giving about 6% increase in lift curve slope and in that way produces more lift as compared to other configurations for the maximum Reynolds number. On the other hand **Saharudin. (2016)** presented the design of a tilting rotor unmanned aerial vehicle (UAV). The main objective for his study was to do structural analysis to size the UAV's wing section. Solidworks and Catia V5 software have been implemented to design and simulation for this research. The load distribution was assumed to be elliptical and the fixed support is at the edge of the wing. As a result of this study it was found that the wing is safe to use in the UAV after doing structural analysis. After doing simulation by using Solidworks 2014 software, it shows that the bending stress is 5.42 MPa. From manual calculation, the theoretical bending stress is found to be 4.26 MPa. There is a small difference with approximately 10% between both values. **Hwang et al. (2007)**, made a cyclocopter propelled by the cycloidal blade system. It is a new concept of VTOL vehicle which has excellent hovering characteristics and low speed forward flight capability. Rotor blades of unmanned cyclocopter with 4 rotors with 16 blades were designed and structural analysis was carried out to reduce drag of each blade and get the high performance for the vehicle. In this study, elliptic airfoil blade was adopted based on the Prandtl's classical lifting line theory to minimize the induced drag hence reduce the required power of cyclocopter rotor system. The geometric parameters of cyclocopter rotor blade system were designed through 2D-CFD analysis. The same airfoil and blade surface area were used for 2D and 3D model. For efficient parametric study the commercial software, STAR-CD and setup of moving mesh method was adopted to simulate the rotation of blades which have periodic pitch angle variation. From this study found that elliptic airfoil achieved low drag, high lift, and maximum displacement and stress of blade were acceptable values. A novel (Unmanned Aerial System) UAS presented by **Trancossi et al. (2015)**, aims to give excellent low speed operations and VSTOL performance. This UAS concept has been named MURALS (acronym of multifunctional unmanned reconnaissance aircraft for low-speed and STOL operation). The main objective of this study was to obtain low speed flight, very short takeoff and

landing, and a control capability by mean of two mobile surfaces in the front canard, which allow changing the pitch angle, and allows full control of the UAV in combination with an ACHEON variable angle of thrust propulsion system. ACHEON project is a new propulsion model specifically conceived to produce a deflection of a synthetic jet without moving parts. A wing section of the series NACA 5 Digit has been selected. The results show that the designed aircraft meets the previous objectives. **Rabbey et al. (2013)** participated in an international competition SAE aero design west, with a unique design of such an UAV. As per competition requirements empty weight of the UAV should be less than 2 lb. and fly with payload as heavy as possible for good scoring. The goal of the project was to develop and show a practical method of building a unique design UAV and also take off, cruise and land it within the specified area given in the competition. The model of the UAV was conducted using Solid Works and tested in wind tunnel. From the test it seen that there is a region of high pressure at the leading edge (stagnation point) and region of low pressure on the upper surface of airfoil and the max C_L for NACA 4412 in the wind testing approximately equals the result of in CFD. Aerodynamic efficiency during flight for the UAV was achieved, and the theoretical design converted into a real aircraft with preliminary design. Various performances for the wings designed with a winglet and without a winglet were investigated by **Salahuddin et al. (2013)**; in their study two different wings were used: an elliptical wing and a short wing. NACA 2412 was used in both cases. The models' geometry was created in the CATIA V5 R19 Software. One of the objectives of this work was to reduce the induced drag formed on wing during the flight operation, the analysis part was done by using the ANSYS Software, The analysis was done by measuring and comparing various aerodynamics characteristics which include drag coefficient C_D , lift coefficient C_L , lift-to-drag ratio L/D , and comparison for affect a winglet on the wing. Thus, after this comparison, they found that the drag decreased and the performance of the aircraft increased with achieved the better efficiency by using elliptic wing with winglet. Computational investigation of inviscid flow over an airfoil was presented by **Kandwal and Singh (2012)**, through experiments using wind tunnel the drag and lift forces were determined. In this work, a computational method was used to deduce the lift and drag properties. The study was done on air flow over a two-dimensional NACA 4412 Airfoil using ANSYS-Fluent to obtain the surface pressure distribution from which drag and lift were calculated using integral equations of pressure over finite surface areas. Results show the value of lift coefficient calculated computationally is 0.654 compared to the experimental value which is 0.649 for invicid flow over the airfoil. While the value of drag coefficient is 0.001 calculate computationally and 0.007 experimentally. Therefore, the CFD simulation results show a good agreement with those of the experiments. As a result, simulation can be considered as a dependable choice to experimental method in determining drag and lift. A set of wings by parametric variation on wing sweep had been constructed. The C_L , C_D and C_m were investigated in steady state CFD of BWB at Mach 0.3 and through wind tunnel experiments on 1/6 model of BWB at Mach 0.1. Pressure variation, Mach number contours and turbulence area was observed from CFD analysis. In investigation, Swept wing was modeled in ansys using NACA 66-012 airfoil. Insertion of key points following the coordinates of NACA 66-012 airfoil at different sections of wing was the first step of modeling. Then, areas were created using these airfoils and therefore a single solid wing was modeled by adding up these areas. Results for lift, drag and pitching moment were obtained from wind tunnel and CFD, therefore compared and results show a good agreement. In this investigation so that delay flow separation had been recommended changing the airfoil of the wing for low speeds to improve the wing and/or increase the surface area of the wing in order to generate high lift, or twisting the wing **Syed et al. (2011)**. The vortex generator is one of the techniques that have been used to control flow separation on a number of aircraft in recent years. in this study investigation about the effects of passive vortex generators (VGs) on Aludra unmanned aerial vehicle (UAV) aerodynamic characteristics had been done, By attached VGs on Aludra UAV's wing in Both experimental and numerical study. The flow measurements are made at various angles of attack by using 3-axis component balance system. In the numerical investigation, the Reynolds-Averaged Navier-Stokes (RANS) code FLUENT 6.3TM was used in the simulations with fully structured mesh with Spalart-Allmaras (S-A) turbulence model. The comparison between the experimental and numerical results shows an acceptable agreement. The parametric study shows that higher maximum lift coefficient was achieved when the VGs were placed nearer to the separation point **ZHEN et al. (2011)**. Analysis for the two-dimensional subsonic flow over 4-digit airfoil NACA0012 at various angles of attack and at a Reynolds number of 3×10^6 was presented by **C. Eleni et al. (2012)**, by solving the steady-state governing equations of continuity and momentum conservation combined with one of three turbulence models [Spalart-Allmaras, Realizable, k- ϵ and k-GD shear stress transport (SST)] the flow was obtained, so that made validation of these models through the comparison of the predictions and experimental measurements for the selected airfoil. The object of the work was to show the behavior of the airfoil at these conditions and to found a confirmed solution method. The computational domain was collected of 80000 cells appeared in a structured way. Calculations were done for constant air velocity changing only the angle of attack for every turbulence model tested. This work highlighted two areas in computational fluid dynamics (CFD) that require further investigation: transition point prediction and turbulence modeling. The laminar to turbulent transition point was modeled in order to get accurate results for the drag coefficient at various Reynolds numbers. The

most suitable turbulence model for these simulations was the k- ω SST two-equation model, because it had a good agreement with the experimental data.

Experimental and CFD analysis of airfoil at low Reynolds number presented by **Sagat et al (2012)**. The determination of lift and drag of airfoil from wind tunnel measurements was discussed for incompressible flow. Calculated the upper and lower surface pressure and velocity of an airfoil is fundamental for calculating the forces on it. Analysis of the airfoil done at low Reynolds no, different angle of attack from 0° to 20° and at maximum velocity 15 m/s. then comparing experimental results and CFD results. The coefficient of pressure was analyzed in the upper and lower surface of the airfoil for the angle of attack varies from 0° to 10° . The pressure on the lower surface of the airfoil was greater than that of the incoming flow stream and as a result of that it effectively pushes the airfoil upward, normal to the incoming flow stream. On the other hand, the components of the pressure distribution parallel to the incoming flow stream tend to slow the velocity of the incoming flow relative to the airfoil, as do the viscous stresses. The coefficient of lift and coefficient of drag of an airfoil depends upon the pressure distribution and velocity distribution of an airfoil. The analysis of the two-dimensional subsonic flow over a NACA 0012 airfoil at various angles of attack and operating at a Reynolds number of $3(10)^6$ had been presented. And the CFD simulation results show close agreement with those of the experiments. From the CFD analysis of the flow over NACA 0012 air foil they found that at the zero degree of AOA there was no lift force generated and if they want to increase amount of lift force and value of lift coefficient, they had to increase the value of AOA. By doing that drag coefficient and drag force also increased but the amount of increment in drag force and drag coefficient was quite lower compare to lift force. **S. Patel et al.(2014)**.

And so from this report and previous studies we have been obtained the drag and lift forces using CFD which can also be determined through experiments using wind tunnel testing. But In experimental setup, the design model has to be placed in the test section and this process is hard and cost more than CFD techniques. So the study had been gone through analytical method then it can be validated by experimental testing.

All of the above shows that there is a convergence of results between experiments and computational methods, thus, the computational studies prove more effective. Also from previous studies we can get the steps required for doing investigations to obtain the max lift to drag ratio, and subsequently getting better best performance of an unmanned aerial vehicles.

Finally outcome from the UAVs survey and the literature study into Rotor/Wing research and development has shown that the CRW-UAV concept is a unique innovative solution for a high-speed unmanned aircraft with vertical takeoff and landing capabilities. Greater understanding of elliptic airfoils could be obtained by utilizing CFD flow solvers to conduct detailed analysis of parameters which have significant effects on aerodynamic performance. Detailed parametric analyses of elliptic airfoils would also aid in studying aerodynamic performance in rotary and fixed-wing flight modes. Therefore, the current study is carried out to understanding of elliptic airfoil at different operating parameters to achieve maximum lift to drag ratio and be employed in the design and development of rotor/wing unmanned aerial vehicles.

2 Computational Model

Computational fluid dynamics, CFD, is a branch of fluid mechanics using numerical analysis and algorithms to solve and analyze problems. When using CFD analysis, it is easy to discover unexpected mistakes which can significantly change the flow field solutions. By comparing results produced from CFD analysis with experimental test results, an analyst can validate their processes and methodology.

Elliptic airfoils possess a unique characteristic, in that, the blunt trailing edge causes flow separation and vortex shedding in the flow field aft of the airfoil, even at low angles of attack, as opposed to conventional airfoils which have a sharp trailing edge. Now that vast improvements have been made in the development of computational flow solving, complex numerical algorithms may be implemented on computational grids. These improvements allow for in depth parametric studies to be conducted at a reasonable cost and time. The computational domain and typical grids considered in this study are shown in Figure (1). Commercial ANSYS-Fluent is selected during the current study to apply the over set grid approach for the structured grid Navier-Stokes method to analyze the aerodynamic performance of a two-dimensional wing cross-section. Analyzing the aerodynamic performance of an airfoil using CFD involves two main processes: grid generation and flow solving. In order to meet the flow solver requirements of simulating a flow field about an elliptic airfoil, an available flow solver which employs the overset-structured grid, Navier-Stokes solution method must be used to carry out the analysis. This flow solving code uses time accurate, Reynolds-Averaged Navier Stokes (RANS) equations. The first step was to create a 2D- surface of the elliptic airfoil. Airfoil surface definition was based upon the 0.16 x chord thickness elliptic airfoil studied by **Kwonand and Park(2005)**, this consisted of a two dimensional ellipse, oriented in the XY-plane, which had a chord length of one unit in the positive X-axis and a maximum thickness of 0.16 units in the Y-axis located at one-half of the chord length along the X-axis, as shown in Figure (1.a). From this surface definition, a surface grid of 250 cells. This point distribution was used so that many

points would be collected in areas of large curvature, where the largest flow gradients will typically exist, as shown in Figure (1.b).

3 Model Validation

In order to ensure the accuracy of computational results, Mesh independent study, turbulence models independent study and validation with the experimental data are performed. In the current study the computational domain is validated by comparing the computational results obtained for a symmetrical, 16% thick elliptic airfoil at a Reynolds number of 3×10^5 with experimental results conducted by **Kwon and Park (2005)**, as indicated in Figures (2 and 3). Figures (2 and 3) indicate the investigation of validation combined with mesh independent study Figure (2), as well as turbulence model independent study Figure (3). The airfoil surface pressure coefficient distribution is used as a key parameter for these studies at AOA= 0° , 2° , 4° , 6° , and 8° . In mesh independent study, four different mesh sizes are tested at AOA= 6° , $V = 25$ m/s and thickness ratio = $0.16 \times$ chord. The results of pressure coefficient distribution over top and bottom airfoil surfaces for the four meshes are effectively grid independent as shown in Figure (2). In addition, a good agreement between the computational and experimental results is achieved. Therefore, mesh 3 (111250 elements), is used for the current investigation to get both good solution accuracy and low computational time.

Moreover, the sensitivity of the computational results to the turbulence models is investigated using four different turbulence models such as standard k- ϵ , RNG k- ϵ , Realizes k- ϵ and SA models at AOA= 0° , 2° , 4° , 6° , and 8° $Re = 3 \times 10^5$ and thickness ratio = $0.16 \times$ chord. The results of the pressure coefficient distribution for all turbulence models and entire range of AOA are very close to each other as shown in Figure (3). The SA model is selected to be used for the current investigation due to its accuracy with the experimental results as indicated in Figures (3.c and 3.d).

4 Boundary Conditions

(BCs) specify the flow variables on the boundaries of the chosen physical model. One of the most challenging an accurate flow field is specification of boundary conditions. In order to complete a flow solving iteration; a boundary condition type must be specified for each grid point on the boundary of the domain. Boundary condition types used in this case are (velocity-inlet, pressure-outlet, viscous adiabatic wall, free-stream/characteristic condition, and plane symmetry). Velocity inlet boundary conditions are used to define the flow velocity, this type of boundary conditions is only suitable for incompressible flows as in this study. A constant, uniform, normal to the boundary flow velocity of 25 m/s was set at the inlet face of the computational domain. Pressure-outlet boundary condition is set at the outlet face of the computational domain with a specific static pressure value. In the present simulation, static pressure was set to be normal to the boundary and to have a zero gauge pressure which means that the outlet face was considered to be opened to the atmosphere. The viscous adiabatic wall boundary condition is applied along the surface of the airfoil. The free stream/characteristic condition is applied to the far-field boundary of the domain. Finally these boundary conditions have been found to work most effectively for flow field simulation about an elliptic airfoil.

5 Turbulence Model

Turbulence models can have a significant influence over flow behavior; there are five types of different turbulence models for predicting turbulent flow, including the Spalart Allmaras (SA) model as i mentioned previously. This model is relatively new, and has achieved much success in accurately predicting free-shear regions (*Introductory FLUENT Notes , 2006*). For this reason, the (SA) model was used in this study. The SA model is a relatively simple one-equation model that solves a modeled transport equation for turbulent viscosity. It was designed specifically for aerospace applications. It is also gaining popularity for turbo machinery applications. In its original form, SA model is effectively a low Reynolds-number model, requiring the viscous-affected region of the boundary layer to be properly resolved in Fluent.

The transported variable in the SA model $\tilde{\nu}$ is identical to the turbulent kinematic viscosity except in the near-wall (viscous affected) region. The transport equation is given by

$$\frac{D\tilde{\nu}}{Dt} = G_{\nu} \left[\frac{\partial}{\partial x_j} \left\{ (\mu + \rho\tilde{\nu}) \frac{\partial \tilde{\nu}}{\partial x_j} \right\} + C_{b2} \rho \left(\frac{\partial \tilde{\nu}}{\partial x_j} \right)^2 \right] - Y_{\nu} + S_{\tilde{\nu}} \quad (1)$$

Where G_{ν} is the production of turbulent viscosity and Y_{ν} is the destruction of turbulent viscosity that occurs in the near-wall region due to wall blocking and viscous damping. C_{b2} are constants and μ is the molecular kinematic viscosity (m^2/s), $S_{\tilde{\nu}}$ is a user-defined source term.

6 Numerical and Visual Analysis

Numerical analysis can be done with simple computer programs; while visual analysis must be conducted using more strong software packages .The primary form of numerical analysis employed in this study is investigation into pressure and force coefficients. Pressure coefficients can be easily calculated from a flow field solution file using fluent. Fluent can then be used to plot the pressure coefficients over the top and bottom surfaces of the airfoil. These plots can be very useful in analyzing and comparing the pressure distributions occurring along the surface of an airfoil for varying flow parameters.

Visual analysis is needed to gain an understanding of boundary layer separation and trailing edge vortex structures. Using visual analysis, one can transform quantitative data into a physical representation of the flow field. The three main plotting techniques employed in this study include: pressure contour plots, velocity contour plots, and pressure coefficient.

7 Governing Equations

The equations that govern the motions of fluid are the Navier-Stokes equations, which are the fundamental principles of fluid dynamics. In this study the modeling is carried out by solving the governing equations for a turbulent flow using fluent code. The governing equations are solved by the two dimensional approach and double-precision solver; option is accepted for all calculations. The following governing equations for flow are solved using computational fluid dynamics (CFD) commercial code, Fluent. The continuity and momentum equations are used to calculate velocity vector (*Introductory FLUENT Notes , 2006*)

Continuity equation

$$\frac{\partial}{\partial x_i}(\rho U_i) = 0 \quad (2)$$

Where U_i is the component of the velocity vector (m/s)

Momentum

$$\frac{\partial}{\partial x_i}(\rho U_i U_j) = -\frac{\partial p}{\partial x_j} + \frac{\partial}{\partial x_i} \left(\mu \frac{\partial U_j}{\partial x_i} \right) \quad (3)$$

Where ρ is the density of the fluid (kg/m³), p is the pressure (Pa) and μ is the fluid viscosity (kg/m.s) and $i, j \in \{1, 2\}$.

8 Results and Discussions

The optimum design of the elliptic wing is the key parameter of the current study to suite the application of UAVs. This study investigates the characteristics of elliptic airfoils for a range of parameters. These parameters include: Reynolds number, thickness ratio, angle of attack, and location of maximum thickness for elliptic wing at max angles.

The Reynolds number was evaluated at values of 1×10^5 , 3×10^5 , 2×10^6 , and 8×10^6 . This range was chosen to identify its effect on aerodynamic performance of rotary and fixed wing flight conditions. Thickness ratio was ranged between 5% and 25%. These airfoil thicknesses are used on UAVs application. Also, angle of attack was evaluated in a wide range from 0° to 18° in order to analyze aerodynamic characteristics up to stall condition. Location of maximum thickness for elliptic wing was evaluated at 30%, 40%, 50%, 60%, and 70% of the chord from the leading edge. The maximum thickness location is investigated at maximum angle of attack to achieve maximum lift to drag ratio.

All of these parameters allow the current study to explore the effects of vortex shedding aft of the airfoil on lift and drag forces. By using the commercial code [ansys-fluent], the continuity, and momentum (eqs. 2 to 3) can be solved and all force (i.e. lift and drag), velocity, and pressure coefficient can be obtained and displayed. Also, visualizations of flow developments including flow separation, vortex separation, and vortex shedding downstream of the airfoil are investigated.

9 Reynolds number effect on airfoil characteristics.

In order to better understand the aerodynamic characteristics of elliptic airfoils, the influence of Reynolds number at angle of attack $\alpha=8^\circ$ on airfoil lift characteristics is evaluated. The canard rotor wing UAV would have a Reynolds number of approximately 2×10^6 during fixed wing flight while flying close to transition speed **Kwonand and Park(2005)**.The Reynolds number observed by the CRW UAV at maximum flight speed would be approximately 8×10^6 **Hui Hu and Yang(2008)**, Therefore; the influence study covered a Reynolds number ranged between 1×10^5 and 8×10^6 on airfoil characteristics the results in Figures (4, 5 and 6). The relation between lift coefficient (C_L) and Reynolds number (Re) is depicted in Figure (4). The maximum lift coefficient =0.73 achieved at $Re=1 \times 10^5$ and decreased with Reynolds number increase so, at $Re=2 \times 10^6$ the lift coefficient reaches to its minimum value of 0.53 and continues constant when $Re > 2 \times 10^6$. The relation between drag coefficient, C_D , and Reynolds number (Re) is shown in Figure (5) at angle of attack $\alpha=8^\circ$. The maximum drag coefficient=0.045 occurred at $Re=1 \times 10^5$ then slightly decreases with Reynolds number increase accordingly the minimum drag coefficient of 0.024 is occurred at $Re= 2 \times 10^6$ and continues constant at this value for $Re > 2 \times 10^6$. The overall performance of an airfoil is better understood by observing the influence of Reynolds number on both lift and drag coefficient using lift to drag ratio (C_L/C_D) as shown in Figure(6). The maximum lift to drag ratio of 21.6 occurs at Reynolds number of 2×10^6 .

9.1 Influence of thickness ratio on airfoil characteristics

The influence of thickness ratio (T_r), on airfoil is another important parameter that should be evaluated. Airfoil lift performance of an elliptic airfoil is evaluated at angle of attack, $\alpha=8^\circ$, and thickness ratios of 5%, 10%, 16%, 20%, and 25% of chord. These thickness ratios are chosen to show changes in aerodynamic performance for airfoils that could be used for different types of UAV applications. As indicated in Figure (7), it is observed that the lift coefficient decreases with increasing thickness. The maximum value of the lift coefficient occurs at 5% and 10% thickness ratio. Above this thickness ratio, lift curve begins to decrease. Figure (8) shows the variation of drag coefficient with thickness ratios ranged from 5% to 25% at angle of attack $\alpha=8^\circ$ and $Re=2 \times 10^6$. The drag decreases with increasing thickness ratio to a minimum value of 0.055 at thickness ratio of 10% and increases again to its maximum value of 0.068. In addition; Figure (9) shows the dependence of lift to drag ratio on thickness ratio between 5% and 25% and the greatest lift to drag ratio of 7.6 is found at thickness ratio of 10%.

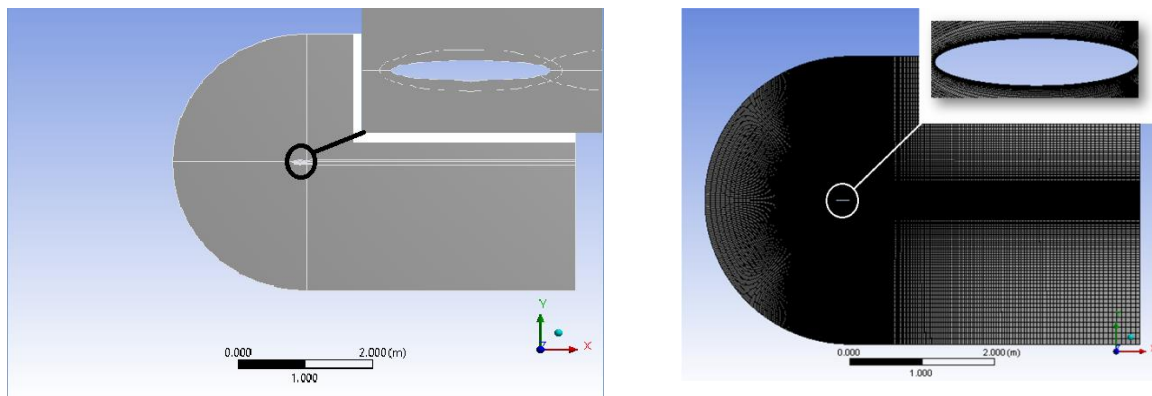
9.3 Influence maximum thickness location on airfoil Characteristics

The effect of maximum thickness location at ($x/c = 30\%$, 40%, 50%, 60%, and 70%) and angle of attack $\alpha=8^\circ$ on airfoil lift characteristics is studied as shown in Figure (10). It is observed that the lift coefficient decreases when the maximum thickness location is near to the airfoil tail. On contrary, the drag coefficient increases due to high and early separation as indicated in Figure (11). The effect of maximum thickness location on the Lift and drag ratio is represented in Figure (12), the greatest lift to drag ratio= 7.98 is observed for a thickness location =30%.

10 Conclusions

In this parametric study, the effects of Reynolds number, thickness ratio, thickness location and attack angle on the aerodynamic characteristics of an elliptic airfoil were investigated. Following are the main conclusions drawn from this investigation:

- A maximum error of about 4% between the model and experimental validation results was achieved.
- Maximum lift to drag ratio of 21.6 occurs at Reynolds number of 2×10^6 and slightly decreased with increasing Reynolds number to its minimum value of 16.02 at Reynolds number of 1×10^5 .
- The thickness ratio has a significant effect on lift/drag ratio. Increasing thickness ratio leads to increase the C_L/C_D ratio to its maximum value of 7.6 at 10% thickness ratio. With higher thickness ratio, C_L/C_D ratio decreased continuously.
- Thickness location ranged from 30% to 70% of chord has a great influence on C_L/C_D ratio, where C_L/C_D ratio decreases when the maximum thickness located towards the airfoil tail. Therefore, the maximum $C_L/C_D=7.98$ is occurred at a thickness location =30%, and the minimum $C_L/C_D=6.92$ at thickness location=70%
- The optimum parameter values to get the best lift and drag were found to be angle of attack 8° , Reynolds number of 2×10^6 , thickness ratio of 10% and thickness location 30%.



(a) The computational domain elliptical airfoil geometry at $t/c=16\%$

(b) Mesh generation for elliptical airfoil at $t/c=16\%$

Figure 1: Geometry and mesh generation for elliptical airfoil at $t/c=16\%$

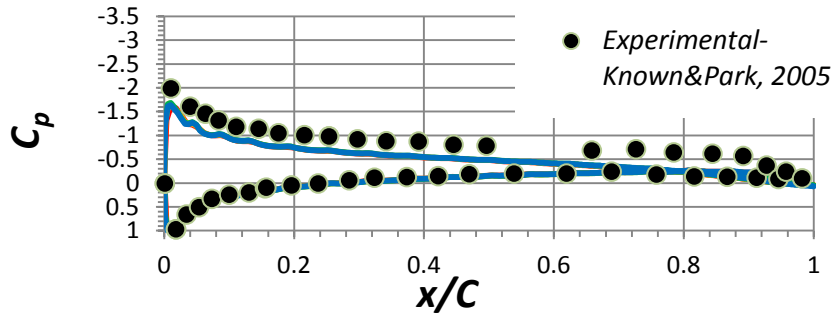
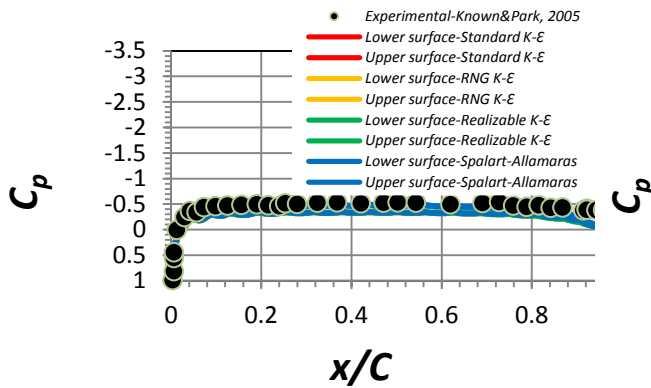
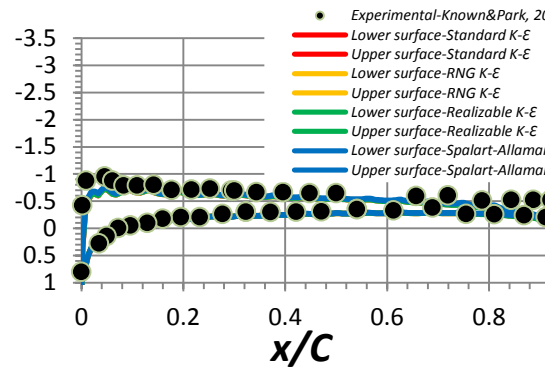


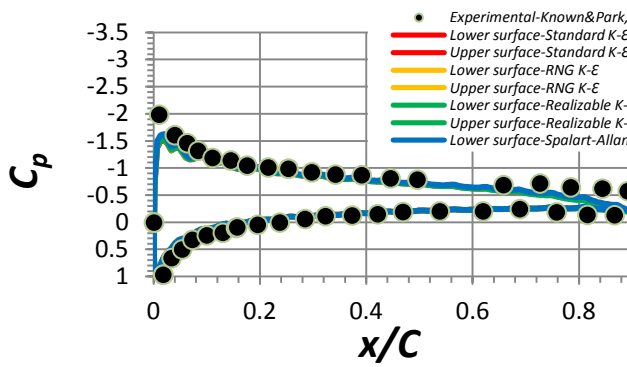
Figure 2: Mesh independence study at $\alpha=0^\circ$ at four levels of mesh



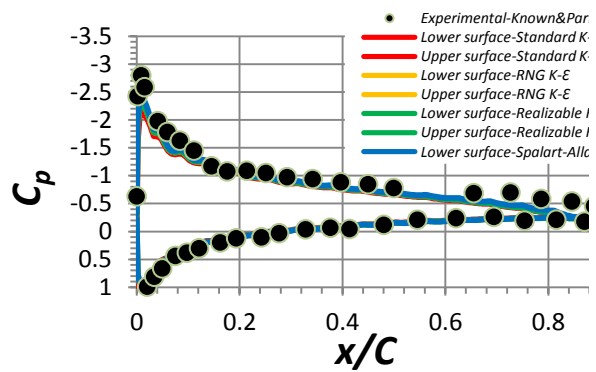
(a): Pressure coefficient at $\alpha=0^\circ$ for different turbulence models



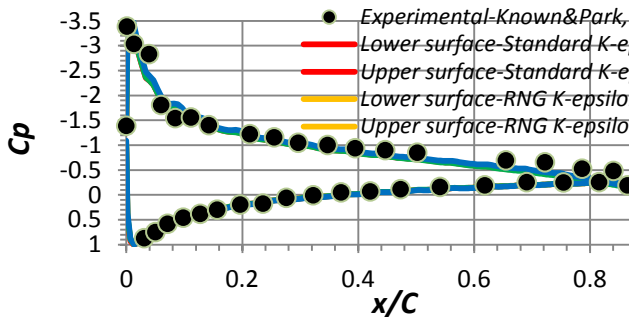
(b): Pressure coefficient at $\alpha=2^\circ$ for different turbulence models



(c): Pressure coefficient at $\alpha=4^\circ$ for different turbulence models



(d): Pressure coefficient at $\alpha=6^\circ$ for different turbulence models



(e): Pressure coefficient at $\alpha=8^\circ$ for different turbulence models

models

Figure 3: The pressure coefficients at different AOA using different turbulence models.

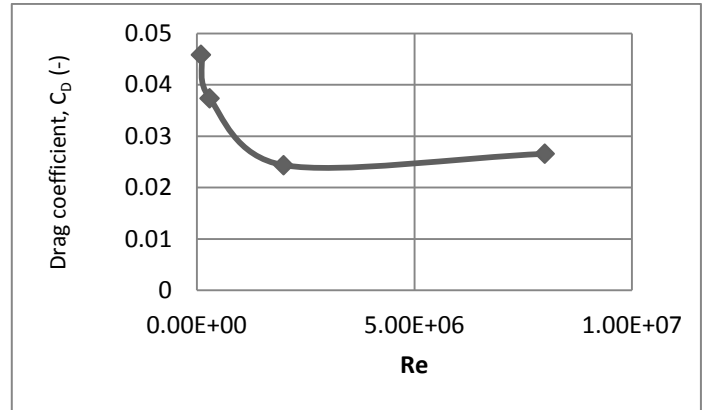
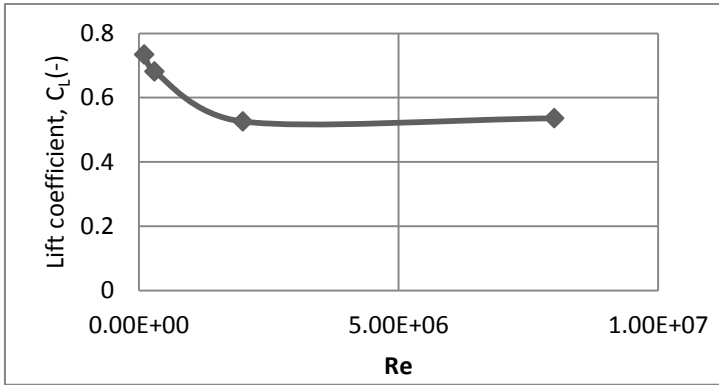


Figure 4: The effect of Reynolds number on airfoil lift coefficient

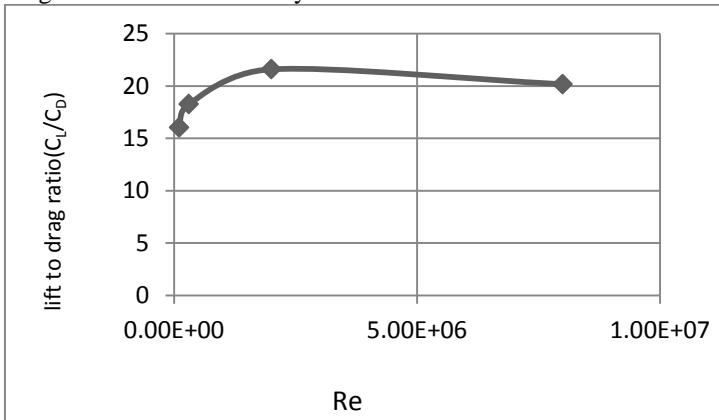


Figure 5: The effect of Reynolds number on airfoil drag coefficient

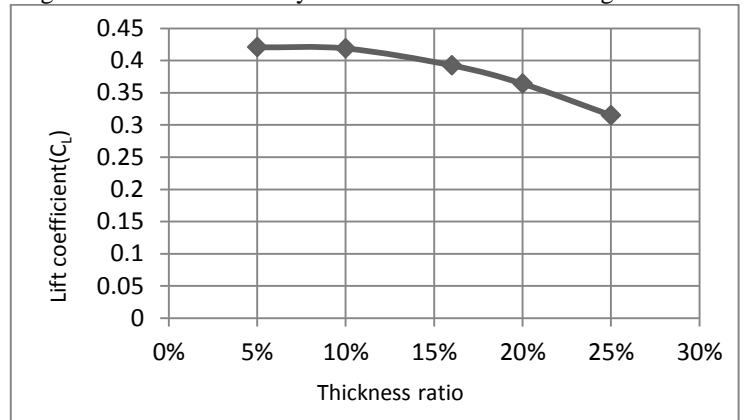


Figure 6: The effect of Reynolds number on airfoil lift to drag ratio

Figure 7: The effect of airfoil thickness ratio on lift coefficient.

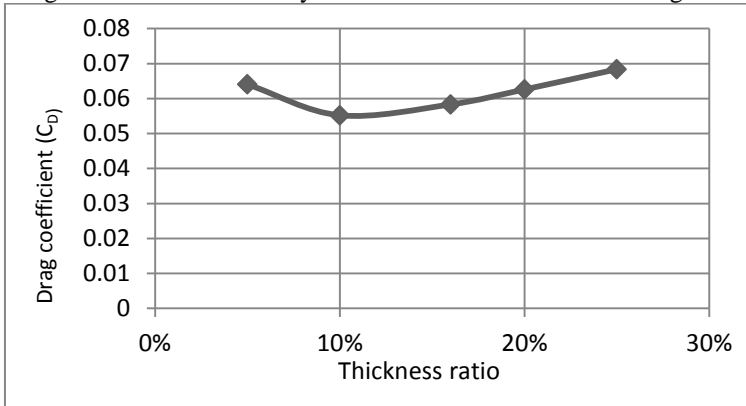


Figure 8: The effect of airfoil thickness ratio on drag coefficient.

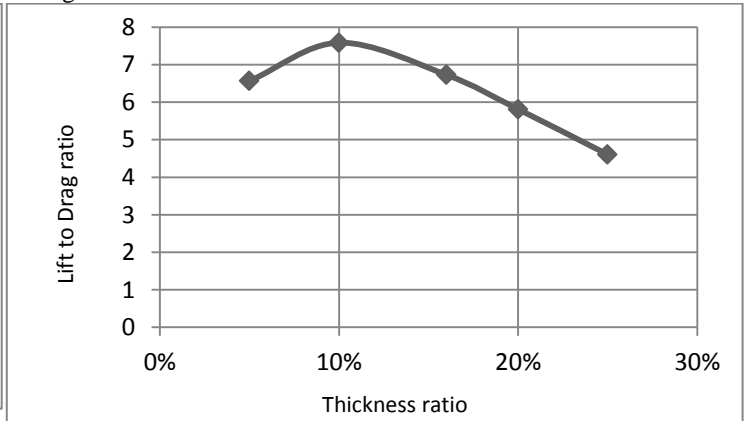


Figure 9: The effect of airfoil thickness ratio on lift to drag ratio.

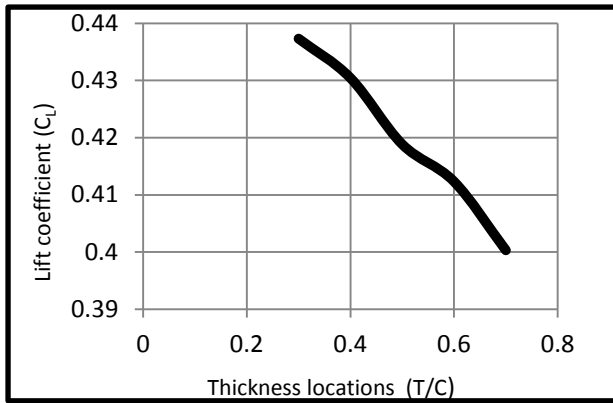


Figure 10: The influence of maximum thickness location on airfoil lift coefficient.

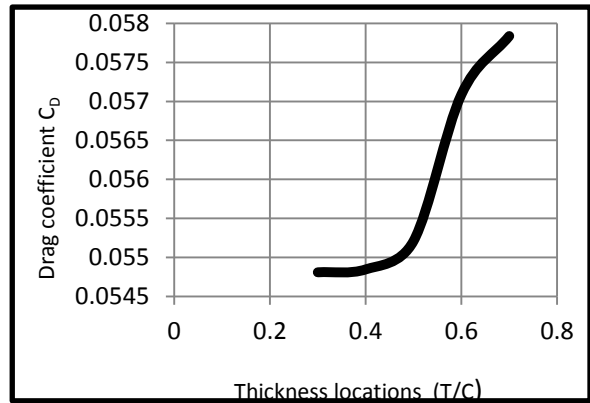


Figure 11: The influence of maximum thickness location on airfoil drag coefficient.

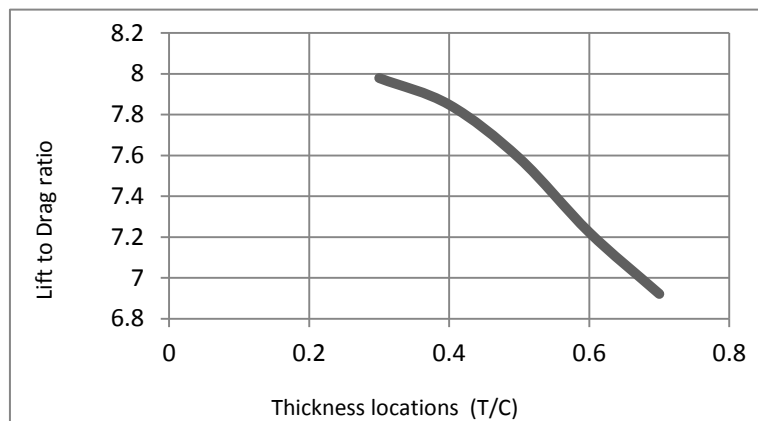


Figure 12: Influence of thickness locations on airfoil max lift/drag ratio characteristics.

Nomenclature

C_P	Pressure Coefficient	(-)
C_D	Drag Coefficient	(-)
C_L	Lift Coefficient	(-)
L/D	Lift to drag coefficient	(-)
T/C	thickness location	(-)
T_R	thickness ratio	(-)
AOA	angle of attack	(-)

References

- **ZHEN, ZUBAIR, and AHMAD. (2011).** Experimental and Numerical Investigation of the Effects of Passive Vortex Generators on Aludra UAV Performance. Chinese Journal of Aeronautics.
- **Trancossi, Bingham, Capuani, Das, Dumas, Grimaccia, Madonia, Pascoa, Smith, Stewart, Subhash, Sunol, and Vucinic (2015).** Multifunctional Unmanned Reconnaissance Aircraft for Low Speed and STOL Operations. SAE Technical Paper 2015-01-2465, doi: 10.4271/2015-01-2465.

- **Syed, Hameed, and Manarvi. (2011).** A Review of Swept and Blended Wing Body performance utilizing experimental, FE and aerodynamic techniques. www.arpapress.com.
- **Salahuddin, Rahman ,and Jaleel . (2013).** a Report on Numerical Investigation of Wings: with and Without Winglet. International Journal of research in aeronautical and mechanical engineering, ISSN (online): 2321-3051. vol.1 I
- **Saharudin. (2016).** Development of tilt-rotor unmanned aerial vehicle (UAV): material selection and structural analysis on wing design. IOP Conf. Series: Materials Science and Engineering 152, Selangor, Malaysia.
- **S. A. Pandya and M. J. Aftosmis. (2001)** Computation of External Aerodynamics for a Canard Rotor/Wing Aircraft.
- **Rabbey, Papon, Rumi, Monerujjaman, and Hasan Nuri. (2013).** Technical Development of Design and Fabrication of an Unmanned Aerial Vehicle. IOSR Journal of Mechanical and Civil Engineering (IOSR-JMCE).
- **R.I Ahmed, A. A. (2016).** Aerodynamics and Flight Mechanics of MAV Based on Coanda Effect. Aerospace Science and Technology.NASA Ames Research Center .Moffett Field, CA 94035
- **Migita, S. A. (n.d.).** Effects of low Reynolds numbers on the aerodynamics of micro air vehicles. Department of Mechanical Engineering University of Hawaii at Manoa Honolulu, HI 96822.
- **Kwon and Park (2005).** Aerodynamic Characteristics of an Elliptic Airfoil at Low Reynolds Number. AIAA 2005-4762.
- **Kandwal and Singh. (2012).** Computational Fluid Dynamics Study of Fluid Flow and Aerodynamic Forces on an Airfoil. ISSN: 2278-0181.
- *Introductory FLUENT notes.* (2006).
- **Hwang, Min, Hee Lee, Han Lee and Kim. (2007)** .Structural design and analysis of elliptic cyclocopter rotor blades. National University, Korea 2Flight Vehicle Research Center, Korea.
- **Hui Hu and Yang. (2008).** An experimental study of the Laminar flow separation on a Low- Reynolds-Number airfoil. Department of Aerospace Engineering, Iowa State University, Ames, IA50011.
- **Hossain, Arora, Jaafar, Iqbal, Arifin. (2007)** Lift analysis of an Aircraft model with and Without Winglet. International Conference on Mechanical Engineering, (IC-ME2007), Dhaka, Bangladesh.
- **C. Eleni, Athanasios and P. Dionissios.(2012).** Evaluation of the turbulence models for the simulation of the flow over a National Advisory Committee for Aeronautics (NACA) 0012 airfoil. Journal of Mechanical Engineering Research Vol. 4(3), pp. 100-111, March 2012,Available online at <http://www.academicjournals.org/JMER>, DOI:10.5897/JMER11.074, ISSN 2141-2383 ©2012 Academic Journals.
- **Sagat, Maneand, and B S Gawali. (2012).** Experimentally and CFD Analysis OF Airfoil at Low Reynolds Number. *ISSN 2278 – 0149 www.ijmerr.com ,Vol. 1, No. 3, October 2012.*
- **Karna S. Patel, Saumil B. Patel, B. Patel, and P. Ahuja. (2014).** CFD Analysis of an Airfoil .international Journal of Engineering Research ISSN:2319-6890(online),2347-5013 Volume No.3, Issue No.3, pp : 154-158